Location-tuned relaxivity in Gd-doped mesoporous silica nanoparticles[†]

Jason J. Davis[*], **Wen-Yen Huang**, and **Gemma-Louise Davies**
Department of Chemistry, University of Oxford, South Parks Road, Oxford, OX1 3QZ, UK

Abstract

In tuning the sub-particle localisation of Gd(III) binding macrocycles within a mesoporous scaffold, nanoparticle contrast agents of unprecedented relaxivity and low Gd(III) loadings can be realised.

Magnetic resonance imaging (MRI) is a powerful non-invasive technique in medical research which becomes considerably more potent when magnetic contrast agents are applied to locally accelerate magnetic relaxation.[1-4] Mesoporous silica structures, including those formed in the micro- and nano-size ranges have been generated by a variety of condensation and template assisted methods.[5-7] Depending on their desired application, additional surface and pore modifications can be achieved by *in situ* co-condensation, post-grafting or imprint coating.[8] In tuning reaction conditions, these modifications can be biased towards either the internal or external surfaces.[9,10] In recent years, significant effort has been invested in the incorporation of resonant contrast enhancing features into mesoporous silica nanoparticles (MSNs),[11,12] which may be additionally modified with other modalities to augment their utility. The relaxation (and hence image contrast) offered by chelate entrapment within particles is generally enhanced in comparison to 'molecular scale' equivalents, an observation commonly assigned to the reduced tumbling rate associated with particles.[13] The efficacy of internal water access in mesoporous materials has been noted experimentally and theoretically and is an important consideration in optimising paramagnetic contrast agent enhancement due to the complex dynamic processes occurring within porous channels.[11,13-17] A number of methods by which Gd-chelates may be loaded into MSNs have been reported, including electrostatically driven layer-by-layer incorporation,[18] direct coupling of the agent using silane chemistry,[12,19,20] or carbodiimide linking through functional groups.[11,13] In this communication, we describe the importance of Gd-chelate localisation and Gd loading in observed T_1-weighted ^{1}H MRI contrast and report the highest r_1 relaxivities achieved to date with particles of this type.

MSNs were prepared herein using an aqueous Stöber technique employing a surfactant template which was subsequently removed to yield an internal hierarchical porous

---

[*]jason.davis@chem.ox.ac.uk; Fax: +44(0)1865 272 690; Tel: +44 (0)1865 275 914.

network.[5,21] The silanol-rich surfaces of the particles were partially aminated by either co-condensing or post-grafting 3-aminopropyltriethoxysilane (APTES). Significantly, amination localisation could be controllably biased internally or externally by performing either time delayed co-condensation (Fig. 1a and b) or post-grafting (Fig. 1c),[9,10] with retention of particle size (66.3 ± 6.6 nm), morphology and pore size (3.2 ± 1.3 nm) (Fig. S1, ESI[†]). These localisations subsequently act as anchor points for gadolinium-1,4,7,10-tetraazacyclododecane-1,4,7-triyl) triacetic acid (Gd-DOTA) attachment by standard chemical means to yield Gd-DOTA-functionalised MSNs (Gd-DOTA-MSNs) (see Experimental procedures and Fig. S2, ESI[†]).

The effects of preparation-tuned Gd-DOTA location bias on ^{1}H spin-lattice MRI relaxivity were observed by monitoring the change in the relaxation rate ($1/T_1$) per mM concentration of Gd on nanoparticulate samples at 7 T (Fig. 1). Notably, delayed co-condensation Gd-DOTA-MSNs exhibited r_1 relaxivities significantly higher (17.14 ± 0.49 mM^{-1} s^{-1} and 33.57 ± 1.29 mM^{-1} s^{-1} for 'short' and 'long delay' reactions respectively) than those prepared by post-grafting (10.77 ± 0.22 mM^{-1} s^{-1}). These relaxivities were, in the most optimised case, more than an order of magnitude greater than observed for molecular Gd-DOTA at the same field (2.01 ± 0.14 mM^{-1} s^{-1}), observations assignable to the markedly reduced rotational flexibility of the chelates when particle confined.[13]

The significant relaxivity enhancements observed for all co-condensation prepared Gd-DOTA-MSNs equate with the internally biased location of the contrast agent chelates in such cases. The behaviour of mobile water confined within the porous networks of mesoporous silica is complex and influenced by molecular interactions with pore walls that reduce diffusive and rotational mobility compared to bulk water.[15-17,22] This restricted innate water mobility, in combination with the internal wall confinement of paramagnetic centres, is expected to lead to markedly increased diffusional (τ_D) and rotational (τ_R) correlation times and altered characteristic water proton residence lifetime (τ_m).[23-25] These effects serve to boost protic contrast and result in the remarkably high relaxivities observed. These confinement effects were additionally probed herein by investigation of the r_1 relaxivity of Gd-DOTA functionalised non-porous silica nanoparticles, prepared by post-grafting. Such particles, with externally Gd-DOTA-loaded surfaces only, exhibit r_1 relaxivities of 9.56 ± 0.47 mM^{-1} s^{-1}, very similar to those observed for post-grafted MSNs.

It is notable that the *delayed* co-condensation preparative technique used here provides a further refinement of relaxivity by enabling not only internal *versus* external control (of doped amine functionalities and hence Gd-chelate units) but also locality within the MSN interior. Specifically, an elongation of the delay leads to a higher probability of functional group distribution nearer to the nanoparticle porous openings, facilitating the correlation time advantages noted above with greater water accessibility and improved ^{1}H relaxivity ('long delay' particles have relaxivities of 33.57 ± 1.29 mM^{-1} s^{-1} at 7 T). Gd-DOTA-MSNs prepared by 'short delay' co-condensation exhibited relaxivities of 17.14 ± 0.49 mM^{-1} s^{-1} at

---

7 T, indicative of more deeply internalised contrast agent groups, unable to undergo efficient water exchange with the external solvent.[11,26]

In addition to maximising contrast performance through localisation, we have examined the potential steric constraints on water access at high levels of Gd-DOTA loading (within particles otherwise optimised by 'long delay' co-condensation preparation). Specifically, samples with different percentage loadings of internalised Gd-DOTA contrast agents have been examined (Fig. 2 and S3, ESI[†]). All Gd-DOTA-MSN samples demonstrated significant relaxation enhancements compared to unbound Gd-DOTA complex in solution, as expected. On increasing loading from 1.37 wt% to 2.07 wt%, relaxivities were observed to drop from 33.57 ± 1.29 mM^{-1} s^{-1} to 19.61 ± 1.51 mM^{-1} s^{-1} respectively, a downward trend which continued as loading was further increased to 3.82 wt% Gd (14.22 ± 0.67 mM^{-1} s^{-1}). We assign these observations not only to the steric effects of increased macrocycle loading on water accessibility[19,26] but also the progressive (sterically driven) bias of macrocycle loading towards the particle external surface at higher concentrations (where the advantages of water and Gd confinement are reduced).

Relaxivity assessments at (more clinically relevant) 3 T fields yielded r_1 values of 39.26 ± 1.29 mM^{-1} s^{-1} for the optimised 1.37 wt% Gd-DOTA-MSNs, a sensitisation which is unprecedented for nanoparticles based on a silica scaffold (prior reported relaxivities of Gd-doped-MSNs span 6.2 to 28.8 mM^{-1} s^{-1} at 3 T; see Table S2, ESI[†]).[12,19,26] Particularly striking in this work is the low level of Gd doping associated with these characteristics. These nanoparticle conjugates additionally exhibit excellent aqueous long-term colloidal, chemical (Fig. S4, ESI[†]) and contrast stability. Furthermore, since Gd loading is controllably internalised, the external particle surface can be biomodified with retention of high contrast (Fig. 2).[27]

Conclusions

In addition to their highly localised physicochemical characteristics and potentially increased blood circulation times, one of the principal advantages nanoparticle contrast agents have over their molecular analogues is their immensely high tunability. We have shown here that even very low levels of Gd-DOTA loading on the walls of mesoporous silica nanoparticles (1.37 wt% Gd, equivalent to 87 μmol g^{-1} of nanoparticles) can be effective in generating T_1 MRI relaxation characteristics with some 20 fold enhancement over free Gd-DOTA ($r_1 = 39.26 \pm 1.29$ mM^{-1} s^{-1} [$1.16 \times 10^6 \pm 3.82 \times 10^4$ per particle] at 3 T and 33.57 ± 1.29 mM^{-1} s^{-1} [$4.94 \times 10^5 \pm 8.03 \times 10^3$ per particle] at 7 T) and markedly higher than in any prior report at comparable field strengths. Central to this has been understanding and optimising the benefits of Gd internalisation on image contrast whilst maximising water exchange. The most promising aspect of utilising nanoparticles in diagnostic or theranostic applications remains an ability to engender high image contrast with additional functionality and low toxicity. We have shown herein that colloidally stable nanoparticles can be precisely engineered to have unprecedented relaxivities and exterior surfaces available for further functionalisation and bio-labelling.

Supplementary Material

Refer to Web version on PubMed Central for supplementary material.

Acknowledgements

Notes and references

1. Huang W-Y, Davis JJ. Dalton Trans. 2011; 40:6087–6103. [PubMed: 21409202]

2. Caravan P, Ellison JJ, McMurry TJ, Lauffer RB. Chem. Rev. 1999; 99:2293–2352. [PubMed: 11749483]

3. Na HB, Song IC, Hyeon T. Adv. Mater. 2009; 21:2133–2148.

4. Davies G-L, Corr SA, Meledandri CJ, Briode L, Brougham DF, Gun'ko YK. ChemPhysChem. 2011; 12:772–776. [PubMed: 21387521]

5. Lin Y-S, Hurley KR, Haynes CL. J. Phys. Chem. Lett. 2012; 3:364–374.

6. Grün M, Lauer I, Unger KK. Adv. Mater. 1997; 9:254–257.

7. Möller K, Kobler J, Bein T. Adv. Funct. Mater. 2007; 17:605–612.

8. Slowing II, Vivero-Escoto JL, Wu C-W, Lin VSY. Adv. Drug Delivery Rev. 2008; 60:1278–1288.

9. Cauda V, Schlossbauer A, Kecht J, Zürner A, Bein T. J. Am. Chem. Soc. 2009; 131:11361–11370. [PubMed: 19722649]

10. Huh S, Wiench JW, Trewyn BG, Song S-Q, Pruski M, Lin VSY. Chem. Commun. 2003:2364–2365.

11. Carniato F, Tei L, Dastru W, Marchese L, Botta M. Chem. Commun. 2009:1246–1248.

12. Taylor KML, Kim JS, Rieter WJ, An H, Lin W, Lin W. J. Am. Chem. Soc. 2008; 130:2154–2155. [PubMed: 18217764]

13. Carniato F, Tei L, Cossi M, Marchese L, Botta M. Chem.-Eur. J. 2010; 16:10727–10734. [PubMed: 20669190]

14. Vallet-Regí M, Balas F, Arcos D. Angew. Chem., Int. Ed. 2007; 46:7548–7558.

15. Takahara S, Sumiyama N, Kittaka S, Yamaguchi T, Bellissent-Funel M-C. J. Phys. Chem. B. 2005; 109:11231–11239. [PubMed: 16852371]

16. Brovchenko I, Geiger A, Oleinikova A. J. Chem. Phys. 2004; 120:1958–1972. [PubMed: 15268330]

17. Milischuk AA, Ladanyi BM. J. Chem. Phys. 2011; 135:174709. [PubMed: 22070319]

18. Kim JS, Rieter WJ, Taylor KML, An H, Lin W, Lin W. J. Am. Chem. Soc. 2007; 129:8962–8963. [PubMed: 17602632]

19. Rieter WJ, Kim JS, Taylor KML, An H, Lin W, Tarrant T, Lin W. Angew. Chem., Int. Ed. 2007; 46:3680–3682.

20. Hsiao J-K, Tsai C-P, Chung T-H, Hung Y, Yao M, Liu H-M, Mou C-Y, Yang C-S, Chen Y-C, Huang D-M. Small. 2008; 4:1445–1452. [PubMed: 18680095]

21. Stöber W, Fink A, Bohn E. J. Colloid Interface Sci. 1968; 26:62.

22. Belorizky E, Fries PH, Guillermo A, Poncelet O. ChemPhysChem. 2010; 11:2021–2026. [PubMed: 20518050]

23. Ananta JS, Godin B, Sethi R, Moriggi L, Liu X, Serda RE, Krishnamurthy R, Muthupillai R, Bolskar RD, Helm L, Ferrari M, Wilson LJ, Decuzzi P. Nat. Nanotechnol. 2010; 5:815–821. [PubMed: 20972435]

24. Fries PH, Belorizky E. J. Chem. Phys. 2010; 133:024504. [PubMed: 20632760]

25. Aime S, Frullano L, Crich SG. Angew. Chem., Int. Ed. 2002; 41:1017–1019.

26. Taylor-Pashow KML, Rocca JD, Lin W. Nanomaterials. 2011; 2:1–14. [PubMed: 24527205]

27. The slight reduction in r_1 observed we assign to non-specific physisorption of proteins onto the nanoparticle surface. W.-Y. Huang, G.-L. Davies and J. J. Davis, manuscript submitted.
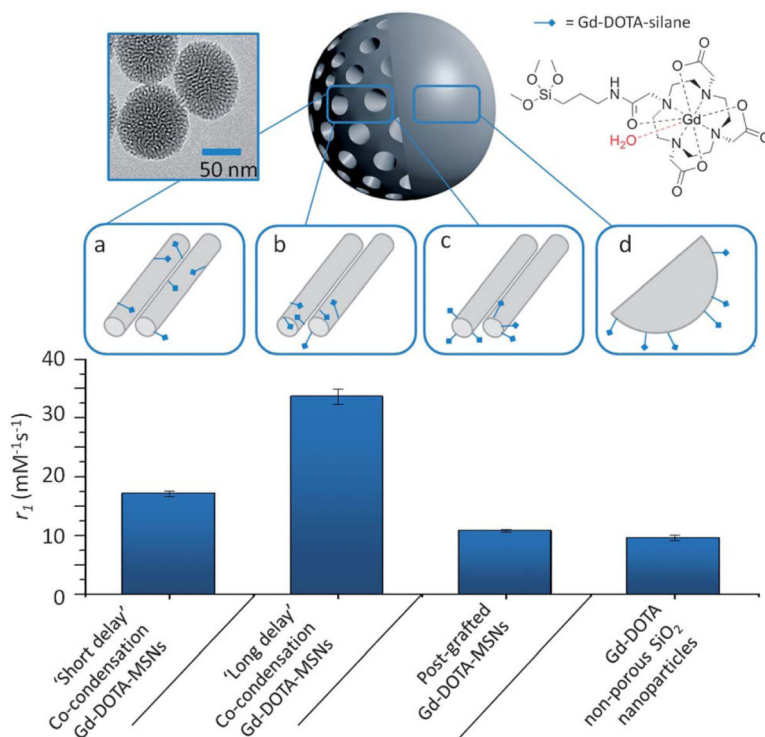
Fig. 1.
Typical transmission electron microscope image and schematic representation of Gd-DOTA-MSNs (66.3 ± 6.6 nm) prepared using (a) 'Short delay' co-condensation, where functionalities are internalised deeply in the structure ($r_1 = 17.14 \pm 0.49$ mM^{-1} s^{-1}), (b) 'Long delay' co-condensation, where functionalities are internalised nearer to the porous openings ($r_1 = 33.57 \pm 1.29$ mM^{-1} s^{-1}) and (c) post-grafting, where functionalities are loaded on external surfaces ($r_1 = 10.77 \pm 0.22$ mM^{-1} s^{-1}). (d) Post-grafted Gd-DOTA-non-porous silica nanoparticles ($r_1 = 9.56 \pm 0.47$ mM^{-1} s^{-1}). The chart displays r_1 relaxivities of corresponding nanoparticle samples, measured at 7 T.
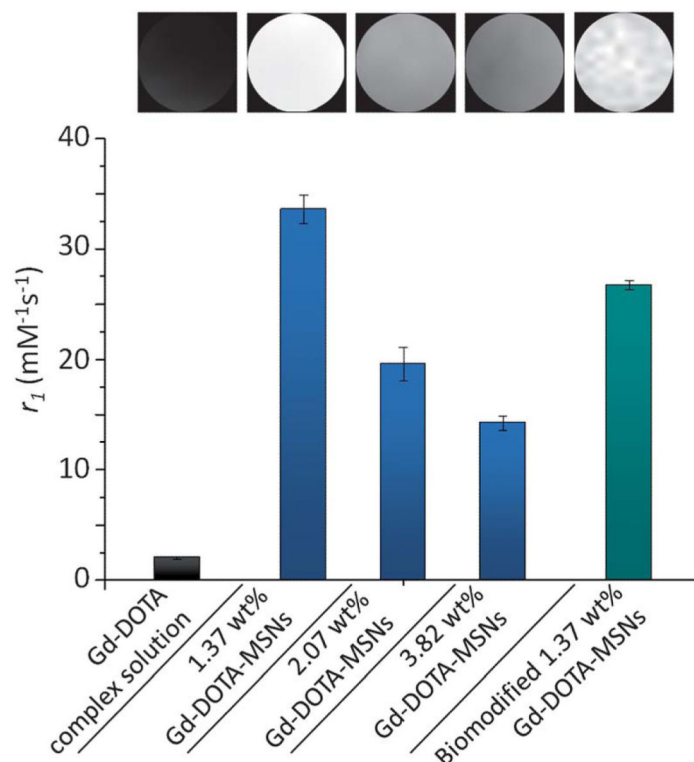
Fig. 2.
^{1}H r_1 relaxivities of Gd-DOTA complex in solution (2.01 ± 0.14 mM^{-1} s^{-1}), Gd-DOTA-MSNs prepared with different percentage Gd loadings (1.37 wt% Gd: 33.57 ± 1.29 mM^{-1} s^{-1}; 2.07 wt% Gd: 19.61 ± 1.51 mM^{-1} s^{-1}; 3.82 wt% Gd: 14.22 ± 0.67 mM^{-1} s^{-1}) and biomodified Gd-DOTA-MSNs (26.69 ± 0.43 mM^{-1} s^{-1}),[27] measured at 7 T. Upper inset shows corresponding T_1-weighted phantom images of aqueous MSN samples with [Gd] 0.04 mM (TR = 30 ms; TE = 5 ms; slice thickness = 2 mm; matrix = 256×256, at 20 ° C).